

Brain Connectivity Predicts Chronic Pain in Acute Mild Traumatic Brain Injury

Noam Bosak, MD,^{1,2*} Paulo Branco, PhD,^{3*} Pora Kuperman, PhD,¹ Chen Buxbaum, MD,^{1,2} Ruth Manor Cohen, MA,¹ Shiri Fadel, BSc,² Rabab Zubeidat, MHA,¹ Rafi Hadad, MD,² Amir Lawen, BSc,¹ Noam Saadon-Grosman, PhD,⁴ Michele Sterling, PhD,⁵ Yelena Granovsky, PhD,¹ Apkar Vania Apkarian, PhD,^{3*} David Yarnitsky, MD,^{1,2*} and Itamar Kahn, PhD ¹

Objectives: Previous studies have established the role of the cortico-mesolimbic and descending pain modulation systems in chronic pain prediction. Mild traumatic brain injury (mTBI) is an acute pain model where chronic pain is prevalent and complicated for prediction. In this study, we set out to study whether functional connectivity (FC) of the nucleus accumbens (NAc) and the periaqueductal gray matter (PAG) is predictive of pain chronification in early-acute mTBI.

Methods: To estimate FC, resting-state functional magnetic resonance imaging (fMRI) of 105 participants with mTBI following a motor vehicle collision was acquired within 72 hours post-accident. Participants were classified according to pain ratings provided at 12-months post-collision into chronic pain (head/neck pain $\geq 30/100$, $n = 44$) and recovery ($n = 61$) groups, and their FC maps were compared.

Results: The chronic pain group exhibited reduced negative FC between NAc and a region within the primary motor cortex corresponding with the expected representation of the area of injury. A complementary pattern was also demonstrated between PAG and the primary somatosensory cortex. PAG and NAc also shared increased FC to the rostral anterior cingulate cortex (rACC) within the recovery group. Brain connectivity further shows high classification accuracy (area under the curve [AUC] = .86) for future chronic pain, when combined with an acute pain intensity report.

Interpretation: FC features obtained shortly after mTBI predict its transition to long-term chronic pain, and may reflect an underlying interaction of injury-related primary sensorimotor cortical areas with the mesolimbic and pain modulation systems. Our findings indicate a potential predictive biomarker and highlight targets for future early preventive interventions.

ANN NEUROL 2022;92:819–833

In the last two decades, advanced neuroimaging technologies have allowed the unraveling of the circuitry underlying chronic pain, with many shared and some disorder-

specific structural and functional brain alternations across divergent clinical populations.^{1–3} It is now acknowledged that the “emotional brain,” including brain structures

View this article online at [wileyonlinelibrary.com](https://onlinelibrary.wiley.com/doi/10.1002/ana.26463). DOI: 10.1002/ana.26463

Received Jan 24, 2022, and in revised form Jul 23, 2022. Accepted for publication Jul 25, 2022.

Address correspondence to Dr Yarnitsky, Rappaport Faculty of Medicine, Technion – Israel Institute of Technology, Haifa, Israel. E-mail: d_yarnitsky@rambam.health.gov.il and Dr Kahn, Department of Neuroscience and Zuckerman Mind Brain Behavior Institute, Columbia University, New York, NY. E-mail: ik2508@columbia.edu

*Noam Bosak and Paulo Branco contributed equally as first authors, Apkar Vania Apkarian, David Yarnitsky, and Itamar Kahn contributed equally to this work as senior authors.

Current address for Amir Lawen and Itamar Kahn: Department of Neuroscience and Mortimer B. Zuckerman Mind Brain Behavior Institute, Columbia University, New York, NY

From the ¹Rappaport Faculty of Medicine, Technion – Israel Institute of Technology, Haifa, Israel; ²Department of Neurology, Rambam Health Care Campus, Haifa, Israel; ³Department of Neuroscience, Northwestern University Medical School, Chicago, IL; ⁴Department of Medical Neurobiology, Faculty of Medicine, The Hebrew University, Jerusalem, Israel; and ⁵RECOVER Injury Research Centre, NHMRC Centre of Research Excellence in Road Traffic Injury Recovery, The University of Queensland, Brisbane, Australia

within the cortico-mesolimbic system, plays a central role in chronic pain, in addition to the well-explored ascending and descending nociceptive pathways.^{3–11} However, understanding of the transition process from acute to chronic pain and the contributing factors that may predict it, which is critical in view of possible preventive therapeutic steps, remains limited.¹²

The nucleus accumbens (NAc) and periaqueductal gray matter (PAG) could reasonably be suggested for the exploration of predictors of acute pain chronification. The NAc is a key structure of the mesolimbic system, involved in reward- and aversion-based learning.^{13,14} It has been extensively linked to chronic pain representation,^{11,15–18} and specifically shown to contribute to the pain chronification process in animal models.¹⁹ Most importantly, enhanced functional and structural connectivity between NAc, medial prefrontal cortex (mPFC) and the amygdala, were demonstrated to precede the onset of subacute lower back pain (LBP) and predict its transition to chronic pain.^{4,9,10}

The dysfunction of the descending pain modulation system, which was shown to convey attention-²⁰ and placebo-related analgesia,²¹ was repeatedly suggested to contribute to pain chronification.^{22,23} The system is commonly clinically assessed using the conditioned pain modulation (CPM) response. Reduced CPM efficiency is evident in different chronic pain populations,²⁴ and was shown to predict chronic musculoskeletal²⁵ and postoperative²⁶ pain, even at the pre-injury stage. The PAG, generally recognized as crucial for nociceptive processing and receiving projections of ascending pain pathways,²⁷ plays a pivotal role in the brainstem's descending pain modulation system.²⁸ PAG's functional properties have been shown to differentiate patients with chronic pain from healthy individuals,^{29,30} and correlate with the individual CPM response,³¹ indicating these properties as potential chronic pain predictors.

In the present study, we focus on mild traumatic brain injury (mTBI) following a motor vehicle collision (MVC), commonly accompanied with whiplash injury,^{32–34} where the majority of affected individuals experience acute pain of defined onset.^{34–37} Of them, 30 to 50% will eventually develop chronic head and/or neck pain,^{35,38,39} for which no adequate treatment exists.⁴⁰ In recent years, a number of studies reported reproducible models intended to identify individuals at risk for future chronic pain following these injuries as candidates for clinical trials of possible preventive interventions.^{36,41,42} However, they hold moderate predictive power and provide limited insights regarding the underlying mechanisms.

We hypothesized that brain function at the acute phase will predict the transition to chronic pain, with NAc and PAG implicated in the process. We used resting-

state functional connectivity (FC), a well-established method for examining brain organization correlates of an individual's traits and state.^{43,44} Here, we report brain FC during the early-acute pain stage (<72 hours from injury) involving NAc, with a complementary parallel pattern concerning PAG, that reflects the tendency to develop long-term chronic pain (12 months post-injury) among individuals with mTBI.

Materials and Methods

Participants

The study protocol was approved by the institutional review board of Rambam Health Care Campus (RHCC) in accordance with the Declaration of Helsinki (No. 0601-14). Individuals suffering from an MVC-induced direct or indirect head and neck injury within the 24 hours preceding visiting the emergency department were recruited as part of a recently completed study.⁴⁵ Participants provided written informed consent prior to any data collection.

Included participants (18–70 years old) reported head and/or neck pain and fulfilled the criteria for mTBI (Glasgow Coma Scale score ≥ 13 upon arrival with no subsequent decline and a transient brain function alteration reported without consciousness loss or shorter than 30 minutes). Exclusion criteria included Hebrew illiteracy, pregnancy, traumatic brain findings on computed tomography (CT) if performed, other major bodily injuries at the present accident, prior chronic head/neck pain requiring regular treatment, head or neck injury in the past year, and convulsive, neurodegenerative, and psychotic spectrum disorders.

Considerable but not complete overlap exists between mTBI and whiplash-associated disorder (WAD) following MVC,³³ based on a similar mechanism of acceleration-deceleration injury, and shared pain distribution and post-concussive complaints.^{38,46,47} To obtain a homogenous participant cohort, we included only individuals that also fulfilled the diagnostic criteria for the 2 milder whiplash injury levels (ie, WAD grade 1–2).⁴⁸ The study population is summarized in Figure 1 and Table 1.

Study Design and Reported Measures

An experimental session was scheduled within 72 hours after injury, during which participants completed questionnaires regarding demographic details, clinical background, and pain-related psychological assessment, and underwent psychophysical tests, electroencephalogram (EEG) recordings, and blood sampling for DNA and RNA analysis, as well as structural magnetic resonance imaging (MRI) and FC measured using resting-state functional MRI (rs-fMRI). An MRI was obtained 1.73 ± 0.77 days on average following the accident, depending on the scanner and participant availabilities.

Participants rated their average and maximal pain intensity during the preceding 24 hours within the area of injury (ie, head and neck), on a numerical pain scale of 0 to 100, which was considered their baseline. Participants were asked to report these ratings once a month for 12 months, using a smartphone

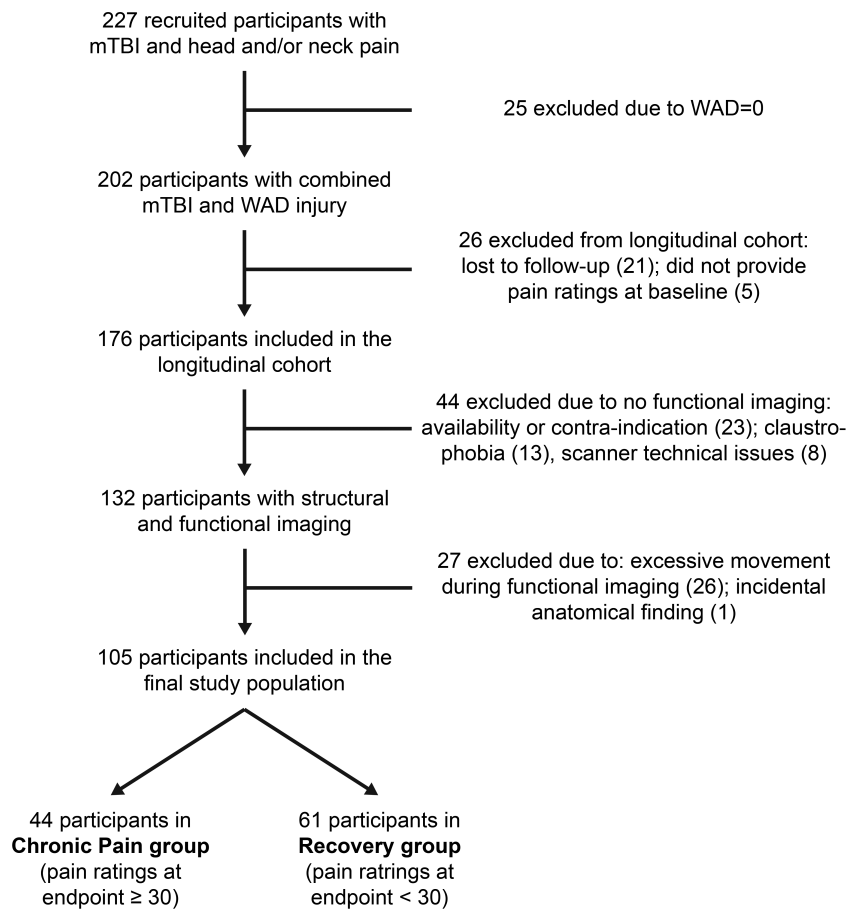


FIGURE 1: Flow chart of study population. mTBI = mild traumatic brain injury; WAD = whiplash-associated disorder.

application, yet, in cases of low compliance, the information was collected via a telephone call.

Group Definition and Clinical/Demographic Statistical Comparison

The pain rating value at a given timepoint was defined as the higher between the reported average head and neck pain intensity, as it most likely represents the ongoing pain within the anatomically and functionally adjacent structures comprising the area of injury.

As pain ratings at the 12-month endpoint did not distribute normally (76 participants [43.18%] reported a zero value), a threshold approach was adopted. Individuals were defined as recovered if their endpoint pain rating indicated no more than mild pain (<30), and as suffering from chronic pain if equivalent to moderate–severe pain.⁴⁹ Between-group comparisons of clinical and demographic parameters were undertaken using Wilcoxon rank sums tests, or independent groups *t* tests and χ^2 tests, as appropriate.

Data Acquisition

Imaging was carried out on a 3T MRI (MR 750, SIGNA 20; GE Medical Systems, Milwaukee, WI) with a 16-channel head/neck/spine coil. The T1 structural images were acquired using a spoiled gradient recall sequence (FA = 12 degrees, FOV = 25.6 × 25.6 cm², 172 slices,

and voxel size = 1 × 1 × 1 mm³). The T2*-weighted fMRI scans were acquired with a whole-brain gradient echo-planar imaging (GE-EPI) sequence (TR/TE = 2000/30 ms, FA = 75 degrees, FOV = 22 × 22 cm², 43 slices, voxel size = 3.4 × 3.4 × 3.4 mm³, and total acquisition time = 10 minutes).

Image Preprocessing and Quality Assurance Criteria

Preprocessing was performed following conventional methods,⁵⁰⁻⁵³ using FSL (FMRIB Software Library version 5.0.1, Oxford, UK) and SPM (Wellcome Department of Imaging Neuroscience, London, UK), and in-house MATLAB (MathWorks, Natick, MA) functions. Steps included removal of the first 4 volumes, slice-dependent time shifts correction (SPM), rigid body motion correction (FSL), and normalization to Montreal Neurological Institute (MNI) template (MNI152) based on affine transformation (FSL). The template normalization step combined motion correction and atlas transformation in one step to yield a motion-corrected volumetric time series sampled at 2-mm cubic voxels. Subsequent resting-state functional connectivity-specific steps included removal of the voxel-wise mean signal and linear trend regression, regression of ventricles, white matter and global average signals, temporal bandpass filtering (0.01–0.1 Hz), and a 6 mm full-width half-maximum Gaussian smoothing. Given the small size of subcortical structures,

TABLE 1. Participants Clinical and Imaging-Related Distribution

	Chronic pain group (n = 44)	Recovery group (n = 61)	Chronic pain group versus the recovery group <i>p</i> value
Age, yr (25–75% range)	36.61 (28–44)	35.18 (27–41)	0.52 ^c
Gender, F/M	25/19	25/36	0.11 ^d
Education, yr (25–75% range)	13.8 (12–15)	14.95 (12–16)	0.054 ^c
Medical background, n (proportion)	13 (0.29)	16 (0.26)	0.71 ^d
Depression diagnosis	0 (0)	2 (0.03)	0.23 ^d
Anxiety diagnosis	1 (0.02)	1 (0.02)	0.81 ^d
Monthly salary, level ^a [n]	2.12 [40]	2.13 [60]	0.93 ^e
WAD grade, 1/2	28/16	47/14	0.2 ^d
Reported injury features, n (proportion)			
Direct impact	9 (0.22)	15 (0.25)	0.62 ^d
Post-traumatic amnesia	0 (0)	2 (0.03)	0.23 ^d
Reported painful body parts outside area of injury ^b during baseline session, n (25–75% range)	1.64 (1–2)	1.48 (1–2)	0.19 ^e
Pain ratings, NPS (25–75% range)			
Baseline	62.2 (49–80)	48.54 (26–70)	0.008 ^{c,f}
3 m	48.8 (22–80) [31]	23.87 (0–46) [53]	0.0004 ^{c,f}
6 m	51.76 (47–70) [36]	20 (0–30) [57]	4.36e-9 ^{c,f}
Endpoint (12 m)	61.84 (48–80)	4.34 (0–8)	/
rs-fMRI motion-related parameters			
Excluded due to excessive motion, n (proportion)	13 (0.23)	12 (0.16)	0.36 ^d
Average displacement (root mean square of motion), mm (25–75% range)	0.055 (0.04–0.07)	0.051 (0.04–0.06)	0.26 ^c
Included frames following scrubbing, n (25–75% range)	235.27 (187–274)	251.41 (230–283)	0.04 ^c

^aAverage monthly salary level in NIS: (1) 0–5 K; (2) 5–10 K; (3) 10–20 K; (4) above 20 K.

^bChosen from a list composed of: chest, abdomen, back, and upper or lower limbs.

^cIndependent groups' *t* test.

^dChi-square test.

^eWilcoxon rank sum test.

^fStatistically significant.

NPS = Numerical Pain Scale; rs-fMRI = resting state functional magnetic resonance imaging; WAD = whiplash associated disorder.

time courses from regions of interest (ROIs) were extracted from unsmoothed data.

As participants were experiencing acute pain, data could be confounded by global motion- and respiratory-related artifacts. Thus, in addition to applying global signal regression, a conservative censoring approach was adopted.^{50,54} Volumes with framewise

displacement over 0.2 mm or delta variation signal over 50 were removed with 1 prior and 2 subsequent volumes, as well as segments lasting fewer than 5 contiguous volumes. Participants (25 [18.9%]) with less than 5 minutes of rs-fMRI after censoring were excluded. The individual average relative root mean square of motion, calculated from 3 rotation and 3 translation parameters

across the entire rs-fMRI acquisition session, was used as covariate of no-interest regressors in group-level analyses.

Predefined Regions of Interest

NAC was defined as a 6-mm radius sphere around the center of gravity coordinates of the relevant subcortical Harvard-Oxford structural atlas mask, which was used previously for FC-based prediction of chronic LBP.^{9,10} Results are reported for both right NAC (rNAC; MNI coordinates [10 12–7]) and left NAC (lNAC; MNI coordinates [–10 12–7]). PAG ROI was defined as a 6-mm radius sphere around the coordinates resulting from a meta-analysis regarding placebo-analgesia-related PAG fMRI activations (MNI coordinates [–1–33 –15]),²⁹ overlapping with previously reported coordinates of the ventrolateral PAG.⁵⁵

Saadon-Grosman et al⁵⁶ recently mapped specific cortical representation of body parts. To probe the spatial specificity, we divided strictly thresholded maps to left/right pre-/post-central gyrus (PreCG/PostCG) strips according to the cortical Harvard-Oxford structural atlas, with each strip further subdivided to 4 somatotopic categories (lips, upper limb, trunk, and lower limb) according to the somatosensory stimuli applied contralaterally to it.

Group-Level Whole-Brain Functional Connectivity Analysis

To produce an individual correlation map, the mean time series from the voxels comprising an ROI was extracted and used to calculate a Pearson correlation coefficient with every other voxel. Fisher's r -to- z transformation was applied before obtaining group mean and difference correlation maps. Age, gender, motion, and baseline pain ratings were entered as regressors in the design matrices of the generalized linear models (GLMs), which were subsequently used to compute group maps using SPM. All group maps, based on 1 and 2-sample t tests, were statistically thresholded at the cluster level for family-wise error (FWE) correction of $p < 0.05$, with initial cluster-forming threshold set at uncorrected voxel-wise $p < 0.001$ and extension >10 voxels.

For follow-up analyses, Fisher's r -to- z transformed correlation coefficients were calculated between an ROI and a 6-mm radius sphere around the reported peak coordinates of significant clusters resulting from the between-group comparisons.

Somatotopic Masks Overlap Quantification

The extent of overlap between the significant clusters resulting from the between-group comparisons and somatotopic lateralized masks was quantified by computing Sørensen–Dice coefficients between them.

Classification Accuracy Using Logistic Regression

To estimate the discriminability between patients who develop chronic pain versus those who recover based on brain parameters, as well as to test whether they explain unique variance beyond that of motion and baseline pain, a sequential logistic-regression model was constructed using scikit-learn.⁵⁷ The first model included the number of frames after scrubbing; the second model added baseline pain ratings; the third model added

the main brain parameters; and the fourth model added post hoc brain findings. A receiver operating characteristic (ROC) curve was calculated for each significant step, and each model was compared to its previous version to probe whether it better discriminates the 2 groups.

Baseline Clinical Parameters' Correlates of Functional Connectivity

Pearson correlation and partial correlation coefficients were calculated using SPSS between the most significant functional link from the logistic regression model and the following clinical parameters elaborated in earlier publications from the same dataset⁴⁵: (1) Psychological questionnaires – Pain Catastrophizing Scale, Pain Sensitivity Questionnaire, Perceived Stress Scale, and Hospital Anxiety and Depression Scale (2 separate scores); and (2) Psychophysical assessment – pain thresholds for electrical, pressure, and heat stimuli, the temperature necessary to induce a heat-pain rating of 50 in °C (Pain50 temperature), heat- and pressure-CPM, as well as mechanical and electrical temporal summation. The procedure was repeated for baseline and endpoint pain ratings. The significance level of each analysis was the false discovery rate (FDR) corrected for multiple comparisons.

Results

Clinical, Demographic, and Imaging-Related Characterization

The study population (see Fig 1) was comprised of 105 individuals, all presented at the emergency department with the maximal Glasgow Coma Scale score of 15, and most of them reported indirect head injury (81 [77.1%]) and were classified as WAD grade 1 (74 [70.5%]). The participants were scheduled for a baseline experimental session during which structural MRI and rs-fMRI were obtained along with baseline pain ratings, followed by subsequent ratings along the year, and at the endpoint of 12 months post-injury (Fig 2A).

According to the described criteria, 44 cohort participants (41.9%) were defined as suffering from chronic pain at the endpoint, in line with both WAD and mTBI literature,^{35,37–39,46} leaving 61 (58.1%) participants in the recovery group. Individuals in the chronic pain group reported significantly higher baseline pain ratings compared to the recovery group (Fig 2B), with the latter demonstrating a trend toward a greater number of years of education. Regarding rs-fMRI motion parameters, the groups only differed in the number of frames after censoring, with the chronic pain group having less volumes. See Table 1 for all summary measures and statistics.

Periaqueductal Gray Matter and Nucleus Accumbens Functional Connectivity

We used rs-fMRI-based FC of both NAC and PAG to assess whether patients who developed chronic pain have

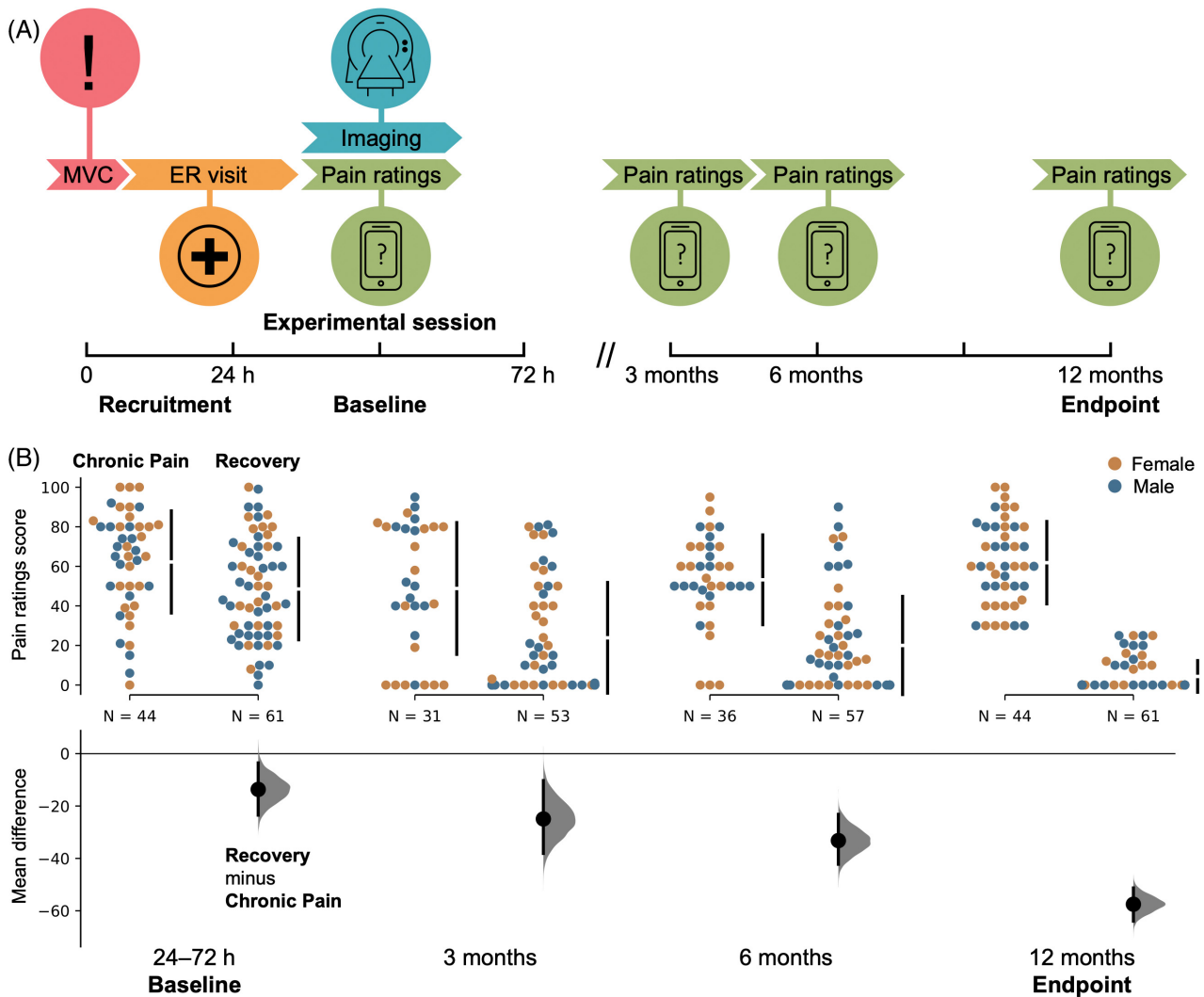


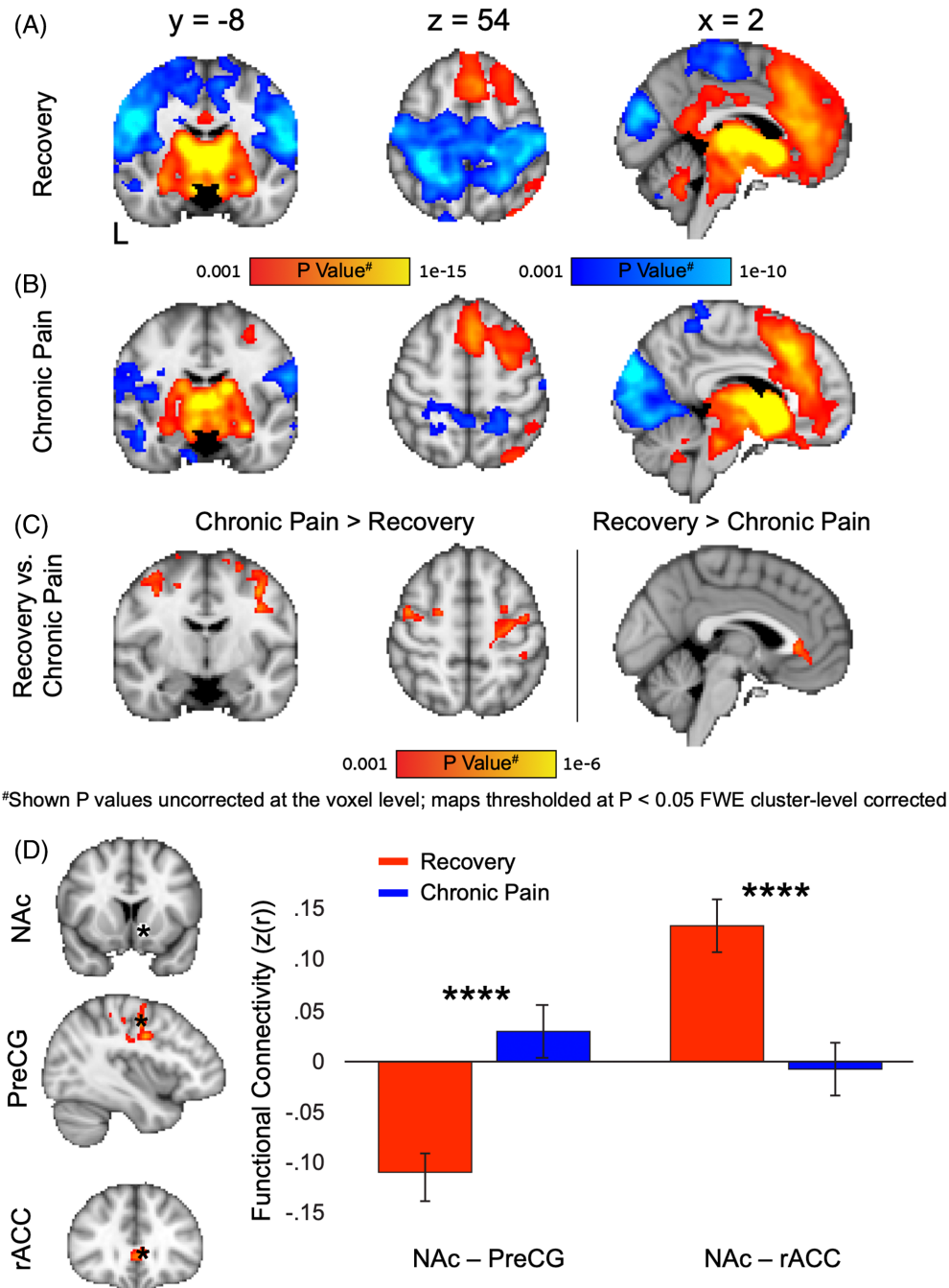
FIGURE 2: Study design and outcome measure distribution. (A) Consenting individuals suffering from mTBI and fulfilling study criteria were recruited at the emergency department and scheduled for an experimental session during the first 72 hours following the MVC, during which structural and resting-state functional MRI scans were obtained. Pain ratings were collected during the session (“baseline”) and later repeated via phone app / call during the following 12 months (“endpoint”). (B) Pain ratings distribution among the recovery and chronic pain groups at the critical timepoints, women are marked in orange and men are marked in cyan. The between-group difference is consistently growing and significant (Student’s *t* test), as detailed in Table 1. mTBI = mild traumatic brain injury; MVC = motor vehicle collision; MRI = magnetic resonance imaging.

distinct patterns of brain connectivity relative to patients that recovered.

When performing whole-brain analysis, we found that both groups’ positive correlation of the whole-brain FC parametric maps for rNac recapitulated previously reported findings, including cortical, striatal, midbrain, and thalamic areas⁵⁸ (Fig 3A, B). A between-group comparison revealed a decreased FC in the bilateral rostral aspect of the anterior cingulate cortex on the border of the perigenual and subgenual rostral anterior cingulate cortex (rACC) for the chronic pain group relative to the recovery group (Fig 3C, D; peak MNI coordinates [6 30 4], $t_{99} = 4.35$, cluster-level $p = 0.017$). Moreover, the negative correlation of the whole-brain FC parametric map of

the recovery group involved bilateral PreCG and PostCG (Fig 3A), a pattern that has been reported,⁵⁸ but was not apparent in the parallel map of the chronic pain group (Fig 3B). This manifested as an increase in FC in PreCG clusters, that marginally involved the PostCG (Table 2), for the chronic pain group relative to the recovery group (see Fig 3C, D; peak MNI coordinates [38–10 48], $t_{99} = 4.9$, cluster-level $p < 0.0001$).

The parallel analyses for lNac provided similar results for between-group comparison, with unilateral increase in FC in the right PreCG cluster (peak MNI coordinates [36 –12 48], $t_{99} = 4.61$, cluster-level $p < 0.0001$) and decreased FC in the left paracingulate gyrus for the chronic pain group relative to the recovery group (peak MNI coordinates



#Shown P values uncorrected at the voxel level; maps thresholded at $P < 0.05$ FWE cluster-level corrected

FIGURE 3: Functional connectivity maps of nucleus accumbens (NAc). Statistical parametric maps for right NAc (rNAc) ROI, positive results in warm shades and negative in blue shades. All the thresholds were set at a cluster level FWE-corrected $p < 0.05$ (based on voxel-wise uncorrected $p < 0.001$, with cluster extent >10 voxels, adjusted for age, gender, movement, and baseline pain ratings). One-sample t tests of (A) the recovery group and (B) the chronic pain group. (C) A 2-sample t test for the chronic pain group versus the recovery group comparison. (D) *Left*, Functional connectivity between the predefined rNAc ROI and the ROIs based on the reported contrast maps' cluster peaks (marked in asterisk, coordinates detailed in text). *Right*, bar plot of the functional connectivity correlation NAc – PreCG and NAc – rACC demonstrating reliable difference across the groups. **** $p < 0.0001$ for independent groups t test. *** $p < 0.001$ for independent groups t test. Error bars represent SEM. Coordinates here and elsewhere refer to the atlas coordinate system of the Montreal Neurological Institute (MNI) template. FWE = family-wise error; NAc = nucleus accumbens; PreCG = precentral gyrus; rACC = rostral anterior cingulate cortex; rNAc = right nucleus accumbens; ROI = region of interest.

$[-18\ 48\ 4]$, $t_{99} = 4.03$, cluster-level $p = 0.016$). Because these results replicate the ones observed for rNAc, we focus on the more significant findings.

The FC parametric map for PAG of the recovery group is consistent with previously reported positive and negative correlations (Fig 4A).^{29–31} Similar findings were

TABLE 2. Overlap Between Different Somatotopic Masks and the Peak Clusters of Reduced Negative Connectivity of NAc and PAG among the Chronic Pain Group

Anatomic area	Somatotopic label	Right mask volume (mm ³)	NAc peak cluster overlap	Sørensen–Dice coefficient	Left mask volume (mm ³)	PAG peak cluster overlap	Sørensen–Dice coefficient
			volume with right mask (mm ³)			volume with left mask (mm ³)	
Motor (precentral gyrus)	Lips	5,480	648	0.09	9,160	592	0.07
	Upper limb	8,248	1,648	0.2 ^a	9,568	976	0.12
	Trunk	3,544	696	0.12	2,152	40	0.01
	Lower limb	3,040	400	0.07	1,736	0	0.00
Somatosensory (postcentral gyrus)	Lips	5,648	696	0.1	5,792	264	0.04
	Upper limb	12,032	16	0.00	10,048	920	0.11
	Trunk	2,696	0	0.00	2,712	1,696	0.36 ^a
	Lower limb	4,280	0	0.00	2,872	160	0.03

^aMaximal overlap ratio per cluster.
NAc = nucleus accumbens; PAG = periaqueductal gray matter.

observed in the chronic pain group for the positive FC correlation only (Fig 4B), resulting in a positive FC correlation overlap between the groups in the caudal PAG-dorsal upper pons, rostral ventromedial medulla, bilateral thalami, and cerebellum (Fig 4C). However, for the negative FC correlation, a between-group comparison revealed decreased FC in the bilateral rACC for the chronic pain group relative to the recovery group (Fig 4D, E; peak MNI coordinates $[-4\ 32\ -2]$, $t_{99} = 4.4$, cluster-level $p = 0.017$), overlapping the result of the parallel analysis of NAc (Sørensen–Dice coefficient of 0.54, Euclidean distance between clusters' centers of gravity 3.16 mm), and indicating an overall greater negative FC correlation in the chronic pain group. Further, we observed an increase in FC in the PostCG clusters, that marginally involve the PreCG (see Table 2), for the chronic pain group relative to the recovery group (Fig 4D, E; peak MNI coordinates $[-32\ -22\ 50]$, $t_{99} = 5.1$, cluster-level $p < 0.0001$), indicating an overall weaker negative FC correlation in the chronic pain group.

Results Projected on Top of a Somatotopic Division of the Sensorimotor Cortex

Previous fMRI studies did not report any consistent coordinates for the somatotopic representation of the neck and head (but not face) areas. Given that these areas are closely localized, yet differentiated in relation to other structures on top of the classical motor and somatosensory Penfield homunculi,⁵⁹ we decided to examine the overlap between

our group-level results and body-part representations of the sensorimotor homunculi. To do so, we used somatotopic brain masks previously published,⁵⁶ while taking into consideration the relation of the expected area of injury representation to other anatomic areas, as illustrated in Figure 5A to C.

When projected on top of the somatotopic masks, it is noticeable that the clusters of increased FC for the chronic pain group relative to the recovery group in the direct between-group comparisons correspond primarily with the bilateral primary somatosensory region trunk masks for PAG (Fig 5D) and the bilateral border area between the primary motor region upper limb and lips masks for NAc (Fig 5E). Interestingly, these findings are in line with the expected area of injury representation on top of the somatosensory and motor homunculi regarding PAG and NAc, respectively (see Fig 5B, C).

Specificity Testing and Thalamic Involvement

The parallel somatotopic results of NAc and PAG between-group comparison suggest a possible shared mechanism, but concurrently raise a question regarding specificity. To further examine whether these regions demonstrated specific functional changes at the network-level, we calculated group parametric maps for the predefined somatotopic masks which overlap with the FC clusters regions reported earlier, that are suggested to represent the area of injury most closely (see Fig 5A, Table 2), rather than the ROIs of the detected regions themselves.

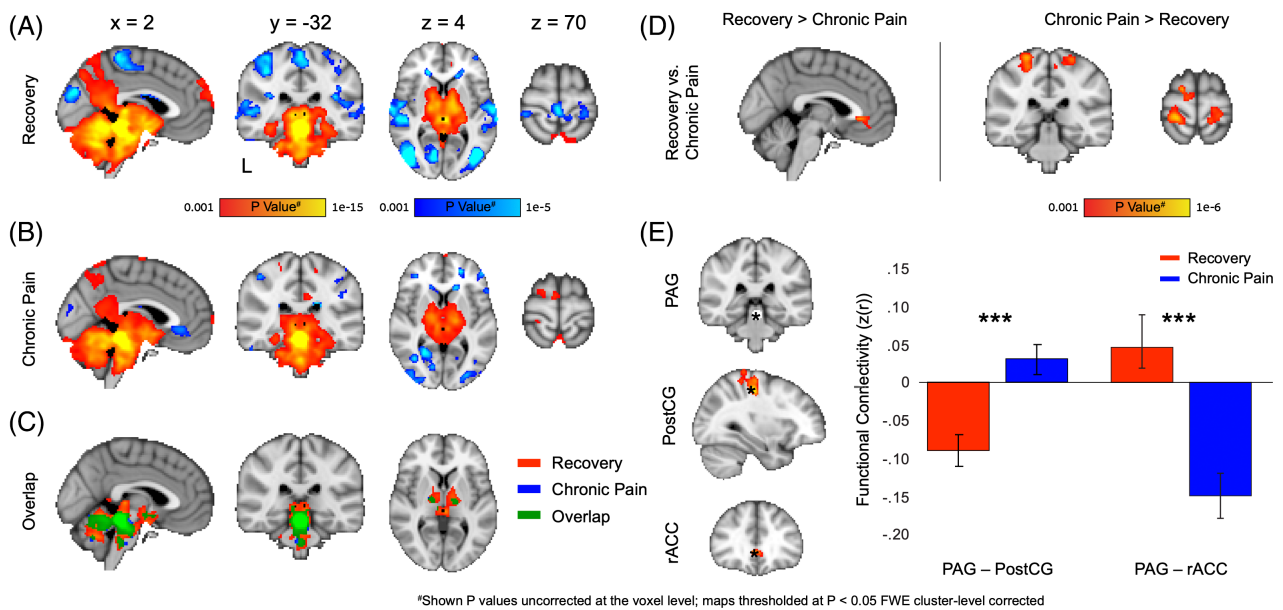


FIGURE 4: Functional connectivity maps of the periaqueductal grey matter (PAG). Statistical parametric maps for PAG ROI, positive correlations are in warm shades and negative in blue shades. Unless mentioned otherwise, all thresholds were set at a cluster level FWE-corrected $p < 0.05$ (based on voxel-wise uncorrected $p < 0.001$, with cluster extent >10 voxels, adjusted for age, gender, motion, and baseline pain ratings). (A) One-sample t tests of the recovery group (ROI coordinates marked as asterisk) and (B) the chronic pain group. (C) To highlight the specificity of the PAG-related positive FC maps, they are presented at more stringent statistical thresholds (voxel-wise FWE-corrected $p < 0.0001$ for sagittal and coronal and <0.001 for axial slices, adjusted for the same parameters): the recovery group (red) on top of the chronic pain group (blue), and their overlapping areas (green shades). (D) A 2-sample t test for the chronic pain group versus the recovery group comparison. (E) *Left*, Functional connectivity between the predefined PAG ROI and the ROIs based on the reported contrast maps' cluster peaks (marked with asterisk, coordinates detailed in text). *Right*, Bar plot of the functional connectivity correlation PAG – PostCG and PAG – rACC demonstrating reliable difference across the groups. *** $p < 0.001$ for independent groups t test. Error bars represent SEM. FC = functional connectivity; PAG = periaqueductal gray; PostCG = postcentral gyrus; rACC = rostral anterior cingulate cortex; ROI = region of interest; FWE = family-wise error; ROI = region of interest.

For the somatosensory component, when contrasting the group maps for the left trunk mask (presumed area of injury somatosensory representation), we found 3 main clusters that showed a significantly decreased negative FC for the chronic pain group relative to the recovery group (Fig 6A). The first cluster consists of the caudal PAG-dorsal upper pons and the rostral ventromedial medulla, the second cluster consists of the ventral tegmental area, the habenula, and the bilateral thalami, and a third cluster involves right globus pallidum. For the motor component, contrast maps for the right motor upper limb mask (presumed area of injury motor representation) revealed 2 clusters which presented a significant decrease in negative FC for the chronic pain group relative to the recovery group (Fig 6B). The first cluster involves the bilateral thalami, the habenula, and left caudate-NAc, and the second cluster consists of the right NAc.

Collectively, these findings suggest specificity to the mesolimbic, descending pain modulation, and sensorimotor systems, including a shared thalamic involvement. The adjacent thalamic clusters' peaks (average MNI coordinates: $[-7 -14 6]$) correspond to the left dorsomedial nucleus of the

thalamus,⁶⁰ and demonstrate a connectivity pattern with the sensorimotor cortex (SMC) which is highly similar to that of PAG and NAc (Fig 6C).

Classification Accuracy Using Motion, Clinical, and Brain Parameters

As the groups differentiated in the number of frames after scrubbing, reported baseline pain ratings at the day of the scan, and FC features, we examined the unique contribution of each parameter by generating a sequential logistic regression model. A model based on the selected motion parameter alone was significant (step 1 $\chi^2 = 4.107$, $p = 0.043$) but provided low accuracy (area under the curve [AUC] = 0.604). Adding baseline pain ratings to the model brought low yet significant improvement (step 2 $\chi^2 = 9.812$, $p = 0.002$; total AUC = 0.693). Adding the 4 hypothesis-driven functional links of NAc and PAG, resulted in a significant improvement (step 3 $\chi^2 = 39.248$, $p < 0.001$; total AUC = 0.873), whereas the thalamic links did not (step 4 $\chi^2 = 3.163$, $p = 0.206$; total AUC = 0.888). In light of the above, and as the motion parameter is of low clinical relevance, we constructed a reduced model

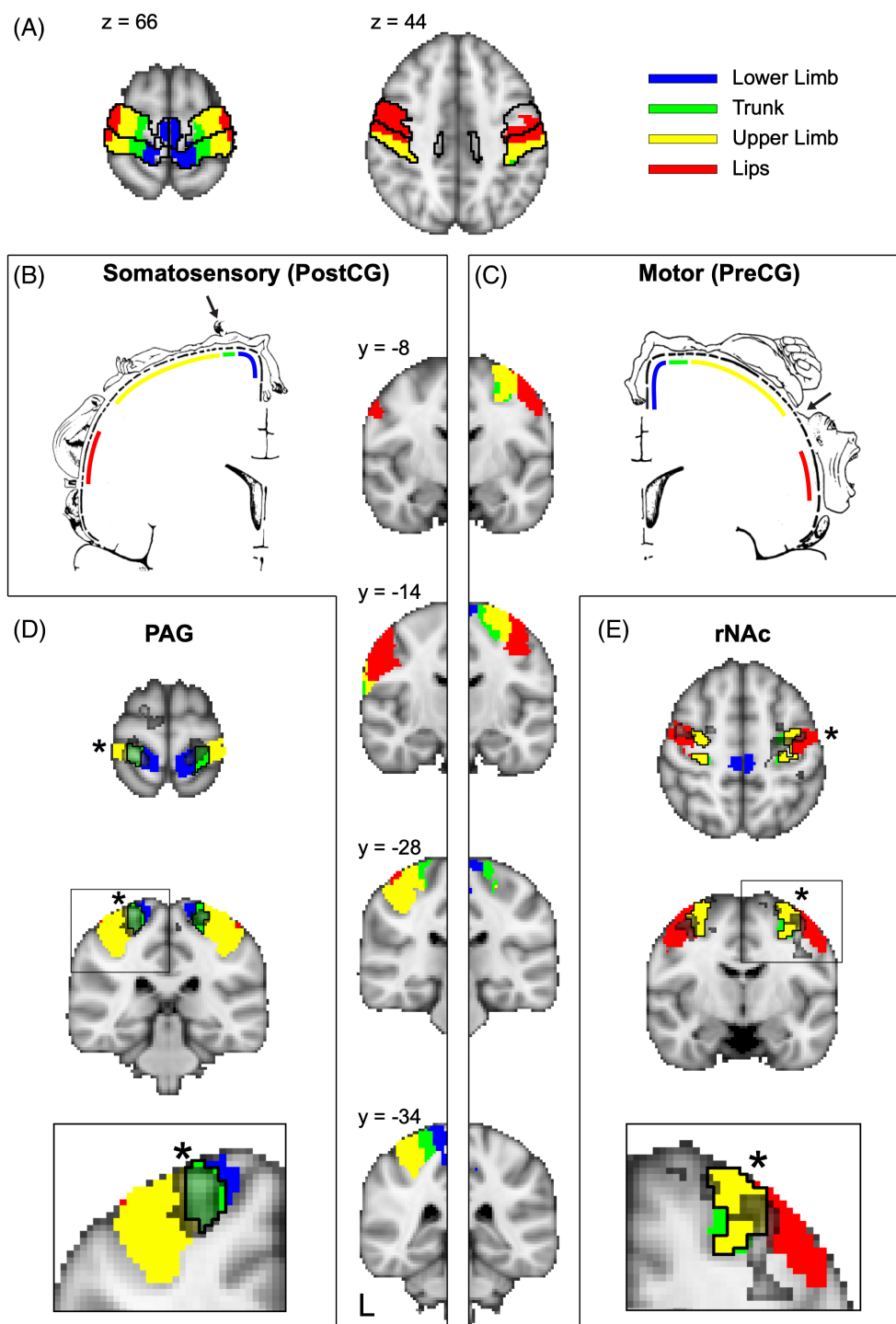


FIGURE 5: Primary motor and primary somatosensory cortical masks with respect to the expected area of injury representation are linked to chronic pain prediction. (A) Somatotopic masks were derived from Saadon-Grosman et al,⁵⁶ in which continuous somatosensory stimulus was applied and later divided to major anatomical categories, as illustrated using schematic color coding within the borders of bilateral PostCG and PreCG (delineated in black), which closely overlap with primary somatosensory and motor cortices, respectively. (B) Classical somatosensory Penfield homunculus illustration (area of injury marked with a black arrow) presented next to PostCG masks on top of the left hemisphere. (C) Classical motor Penfield homunculus illustration (area of injury marked with a black arrow) presented next to PreCG masks on top of the right hemisphere. The significant clusters from the 2-sample *t* test maps for the chronic pain group > the recovery group comparisons presented earlier (statistical information detailed in the relevant figures), now in grayscale and partially transparent, asterisk marking the peak clusters: (D) PAG's map (as in Fig 4D) overlaid on PostCG somatosensory homunculus masks, overlaps mainly with the bilateral representation of the trunk. (E) Right NAc's map (as in Fig 3C) overlaid on PreCG motor homunculus masks, located bilaterally on the border between the masks representing the lips and upper limb. FWE = family-wise error; rNac = nucleus accumbens; PAG = periaqueductal gray; PostCG = postcentral gyrus; PreCG = precentral gyrus.

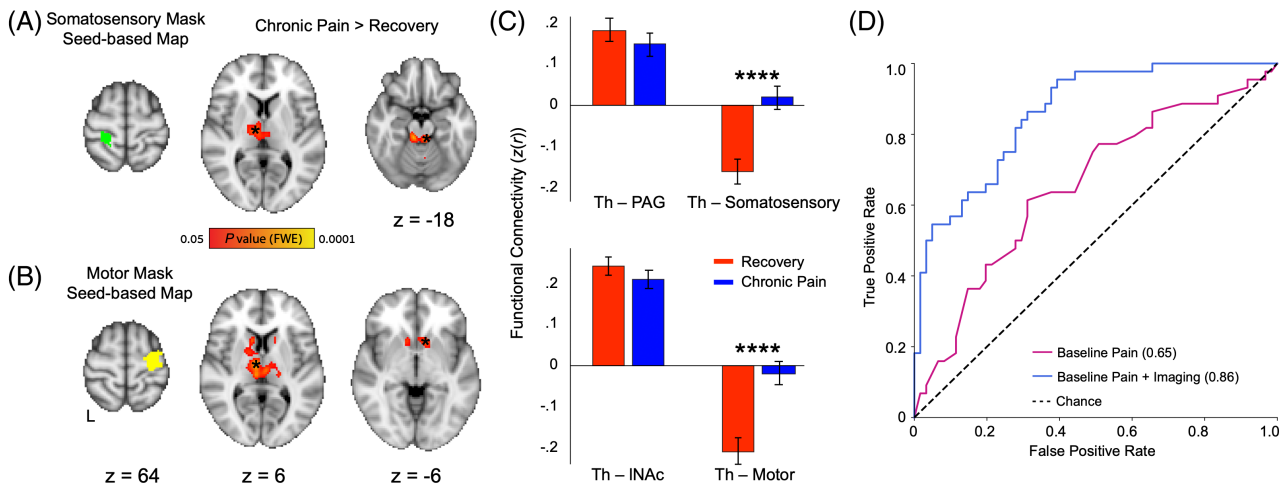


FIGURE 6: Thalamic involvement and classification accuracy of logistic regression models. The 2 predefined somatotopic masks were selected based on the degree of overlap with the prior analyses (Table 2), and are suggested to represent the area of injury most closely. We present the significant clusters resulting from the 2-sample t test of the chronic pain group > the recovery group comparison (thresholds were calculated based on $p = 0.001$, cluster-level FWE-corrected $p < 0.05$, voxel extent ≥ 10 , adjusted for age, gender, movement, and baseline pain ratings) for these 2 masks: (A) Left: PostCG trunk mask (“Somatosensory mask”; green), involving caudal PAG-dorsal upper pons and bilateral thalami; and (B) right PreCG upper limb mask (“Motor mask”; yellow), involving bilateral NAc and thalami. Marked with asterisks are the thalami clusters’ peaks. (C) Functional connectivity between the selected somatotopic masks and the unbiased ROIs based on the cluster peaks from the prior panels. **** $p < 0.0001$ for independent groups t test. (D) Receiver operating curves for the logistic regression models gradually adding baseline pain and functional connectivity values as features (detailed in the text), showing the significant and prominent role of the aforementioned. FWE = family-wise error; NAc = nucleus accumbens; PAG = periaqueductal gray; PostCG = postcentral gyrus; PreCG = precentral gyrus; ROI = region of interest.

(Fig 6D) additively including only baseline pain (step 1 $\chi^2 = 7.061$, $p = 0.008$; AUC = 0.655), and the 4 hypothesis-driven links, which still provided excellent classification accuracy (step 2 $\chi^2 = 40.276$, $p < 0.001$; total AUC = 0.862), with only 3 significantly contributing variables: NAc-PreCG FC ($B = 8.597$, $p = 0.003$), baseline pain ($B = 6.217$, $p = 0.013$), and NAc-rACC FC ($B = 4.345$, $p = 0.037$).

Psychological and Psychophysical Correlates of Functional Connectivity

Finally, we sought to identify clinical correlates of the functional link most significantly associated with the chronic pain outcome. To do so, we computed the correlation coefficients between NAc-PreCG FC and pain-related psychological and psychophysical parameters collected at the same baseline session. This functional link significantly correlated with: (1) pain sensitivity questionnaire score (PSQ; $r = 0.269$, FDR-corrected $p = 0.045$); and (2) Pain50 temperature ($r = -0.242$, FDR-corrected $p = 0.045$). The other clinical parameters, detailed in the Methods section, did not demonstrate significant correlation. No significant correlations were evident in our study population between the same clinical parameters and endpoint pain ratings after controlling for multiple comparisons, nor between the FC intensity and

baseline pain ratings ($r = 0.119$, $p = 0.229$). Nonetheless, as some of those clinical parameters were shown to correlate with acute pain intensity in our research population,⁴⁵ we also computed partial correlation coefficients controlling for the baseline pain ratings, which remained significant for both the PSQ and Pain50, as well as electrical pain threshold (p values 0.263, -0.321 , and -0.267 , and FDR-corrected p values: 0.026, 0.013, and 0.026, respectively).

Discussion

We report on a functional connectivity pattern in the early-acute stage after injury that indicates future long-term chronic post-traumatic head and/or neck pain. Individuals whose acute pain transitioned into chronic pain exhibited baseline reduced negative correlation between NAc and an area within the motor cortex corresponding with the expected representation of the area of injury, a functional link that correlates with baseline clinical measures of pain sensitivity. The PAG demonstrated a complementary pattern with the somatotopically-relevant area within the somatosensory cortex. Both structures share reduced connectivity with a specific location in the rACC in these patients. The results are of clear specificity to the sensorimotor system on the one hand, and the mesolimbic

and descending pain modulation systems on the other, potentially conveyed through the thalamus.

The fact that NAc FC was associated with the transition to chronic pain in our study is not surprising, given that in the largest longitudinal studies to date it was shown to be predictive of pain chronification in subacute LBP.^{4,9,10} An interesting aspect in these studies is that they show, over time, that pain-related functional activity remains similar in the cortico-mesolimbic system, whereas it shifts from sensorimotor to emotional-limbic brain representations during the transition.^{4,11} Indeed, functional and structural brain alternations across several chronic pain populations involve mainly brain areas within these systems.^{3,6,7} This concept is in line with the long-standing view regarding NAc,⁶¹ that emphasizes its role not merely in reward/aversion encoding for reinforcement learning, but rather as a modulator of motor behavior based on sensory and limbic information. We suggest that the reduced negative correlation between NAc and the primary motor cortex observed among individuals prone to chronic pain in our study may reflect a loss of an inhibitory interaction between the mesolimbic and sensorimotor systems that perhaps contributes to the transition to chronic pain.

Both PAG and NAc demonstrated FC changes involving the injured head and neck representation on the primary somatosensory and motor cortices, respectively. These rather specific somatotopic profiles do not correlate with acute pain intensity. However, NAc-SMC FC does correlate with pain sensitivity-related parameters collected at baseline, some of which previously reported to correlate with acute pain intensity,⁴⁵ whereas none seem to be predictive of the eventual chronic pain intensity. The thalamus displayed similar connectivity pattern with the SMC as PAG and NAc, but those links did not provide significant added value to the classification. This, alongside the lack of direct structural connection between PAG or NAc and the SMC, perhaps implies that in this context the thalamus serves as a “relay station.” Increased FC of SMC to the PAG and/or thalamus, with somatotopic specificity in some of the cases, was previously observed in the presence of postherpetic neuralgia,⁶² LBP,⁶³ and fibromyalgia, where it has been shown to be reversible following successful intervention.⁶⁴

It seems reasonable to view these FC axes as part of the same complex network, perhaps linked by the reported circuit composed of NAc, PAG, and the habenula, and structurally linked to the SMC through the thalamus, which is presumably involved in pain processing.⁶⁵ Moreover, the somatotopic specificity of our findings within this network implies that they represent some reactive behavioral pattern, yet they do not simply correlate with acute pain intensity. We may cautiously suggest that these functional links perhaps reflect the integration of nociceptive and emotional features of acute

pain, possibly contributing to the somatosensory and motor learning involved in pain chronification.

The rACC is often regarded as a sub-area of the mPFC. Both areas were linked to the mesolimbic and pain modulation systems and attributed to neuropsychiatric pathophysiology,^{14,66} and even exhibit shared fundamental FC changes across different pain states.^{8,67} Our study demonstrated reduced FC of NAc and PAG to a specific rACC region in patients with acute post-traumatic pain who did not recover. Reduced PAG-rACC FC at rest seems to characterize both pronociceptive healthy individuals,^{31,67} and populations affected by postherpetic neuralgia and episodic migraine.^{62,68} However, patients with chronic LBP display increased PAG-mPFC³⁰ and NAc-mPFC¹⁰ FC compared with healthy individuals, and the structural connectivity between the aforementioned structures was previously shown to reflect a predisposing factor for their chronic pain.¹⁰ These apparently opposing findings could be attributed to a difference in the clinical conditions and timelines between the studies, or possibly the structural and functional differences between mPFC and rACC.⁶⁹ Altogether, we provide further evidence of the centrality of mPFC/rACC to pain persistence, but whether these FC features precede the injury could not be adjudicated from our data.

The vast majority (89%) of the recruited patients with mTBI in our cohort also fulfilled the diagnostic criteria for WAD, perhaps supporting the notion that referred neck pain contributes to post-traumatic headache.^{32–34,40} Whether co-dependent or not, chronic post-traumatic head and/or neck pain are common negative sequela of the highly prevalent injuries of mTBI and WAD following an MVC.^{35,38,46} Our findings, although still requiring external validation, suggest that the combination of subjective pain report with FC-related findings collected at the early-acute stage, may provide higher accuracy in identifying individuals at risk for chronic pain (AUC = 0.862) than previously reported models based on multiple clinical measures (AUC = ~0.7).^{36,41,42} A model incorporating clinical and imaging-based measures is expected not only to improve the predictive capacity, but also to enrich our understanding of the complex mechanisms underlying the chronification process.

Limitations of our study include that it was designed to address the transition from acute to chronic pain, hence, it did not include healthy individuals, and some information regarding other clinical outcome measures, such as post-concussive or post-traumatic stress disorder-related status were not collected systematically. Excessive movement during an MRI scan is a built-in limitation when dealing with acutely injured individuals, requiring frame censoring and high ratio of participant exclusion, but hopefully was well addressed.

Conclusions

In conclusion, our study demonstrates that individuals who eventually developed chronic pain following mTBI could be differentiated from the ones who recover well in the very early-acute state, based on connectivity of the sensorimotor system and PAG and NAc. These findings, if validated, may identify patients at risk as prospects for exploring early use of existing interventions. Moreover, future research of the implicated mechanism can potentially establish new therapeutic pathways for the prevention and relief of chronic pain.

Acknowledgments

This work was supported by the Office of the Assistant Secretary of Defense for Health Affairs under award W81XWH-15-1-0603. Opinions, interpretations, conclusions, and recommendations are those of the authors and are not necessarily endorsed by the Department of Defense. Role of Funder was only monetary in nature.

The authors thank the members of Kahn laboratory, Ornit Nahman, Eyal Bergmann, Gil Zur, and Rotem Paz, for their assistance in data analysis and manuscript preparation. We thank Daniela Lichtman for assistance with technical and language editing of the manuscript.

Author Contributions

D.Y., A.V.A., Y.G., P.B., N.B., and I.K. contributed to the conception and design of the study. N.B., P.B., P.K., C.B., R.M.C., S.F., R.Z., R.H., A.L., N.S.G., M.S., Y.G., A.V.A., D.Y., and I.K. contributed to the acquisition and analysis of data. N.B., P.B., D.Y., and I.K. contributed to drafting the text and preparing the figures.

Potential Conflicts of Interest

The authors do not have any conflicts of interests or commercial relationships related to this study.

References

- Cauda F, Palermo S, Costa T, et al. Gray matter alterations in chronic pain: A network-oriented meta-analytic approach. *NeuroImage Clin* 2014;4:676–686. <https://doi.org/10.1016/j.nicl.2014.04.007>.
- Mansour A, Baria AT, Tetreault P, et al. Global disruption of degree rank order: A hallmark of chronic pain. *Sci. Rep* 2016;6:1–17. <https://doi.org/10.1038/srep34853>.
- Brandl F, Weise B, Mulej Bratec S, et al. Common and specific large-scale brain changes in major depressive disorder, anxiety disorders, and chronic pain: a transdiagnostic multimodal meta-analysis of structural and functional MRI studies. *Neuropsychopharmacology* 2022;47:1071–1080. <https://doi.org/10.1038/s41386-022-01271-y>.
- Hashmi JA, Baliki MN, Huang L, et al. Shape shifting pain: chronicification of back pain shifts brain representation from nociceptive to emotional circuits. *Brain* 2013;136:2751–2768. <https://doi.org/10.1093/brain/awt211>.
- Schwartz N, Temkin P, Jurado S, et al. Decreased motivation during chronic pain requires long-term depression in the nucleus accumbens. *Science* 2014;345:535–542. <https://doi.org/10.1126/science.1253994>.
- Barroso J, Wakaizumi K, Reis AM, et al. Reorganization of functional brain network architecture in chronic osteoarthritis pain. *Hum Brain Mapp* 2021;42:1206–1222. <https://onlinelibrary.wiley.com/doi/abs/10.1002/hbm.25287>.
- Huang S, Wakaizumi K, Wu B, et al. Whole-brain functional network disruption in chronic pain with disk herniation. *Pain* 2019;160:2829–2840. <https://journals.lww.com/10.1097/j.pain.0000000000001674>.
- Yu S, Li W, Shen W, et al. Impaired mesocorticolimbic connectivity underlies increased pain sensitivity in chronic low back pain. *Neuroimage* 2020;218:116969. <https://doi.org/10.1016/j.neuroimage.2020.116969>.
- Baliki MN, Petre B, Torbey S, et al. Corticostriatal functional connectivity predicts transition to chronic back pain. *Nat Neurosci* 2012;15:1117–1119. <https://doi.org/10.1038/nn.3153>.
- Vachon-Preseuse E, Tetreault P, Petre B, et al. Corticolimbic anatomical characteristics predetermine risk for chronic pain. *Brain* 2016;139:1958–1970. <https://doi.org/10.1093/brain/aww100>.
- Baliki MN, Geha PY, Fields HL, Apkarian AV. Predicting value of pain and analgesia: nucleus accumbens response to noxious stimuli changes in the presence of chronic pain. *Neuron* 2010;66:149–160. <https://doi.org/10.1016/j.neuron.2010.03.002>.
- Cohen SP, Vase L, Hooten WM. Chronic pain: an update on burden, best practices, and new advances. *Lancet* 2021;397:2082–2097. [https://doi.org/10.1016/S0140-6736\(21\)00393-7](https://doi.org/10.1016/S0140-6736(21)00393-7).
- Knutson B, Adams CM, Fong GW, Hommer D. Anticipation of Increasing Monetary Reward Selectively Recruits Nucleus Accumbens. *J Neurosci* 2001;21:1–5. <https://doi.org/10.1523/JNEUROSCI.21-16-j0002.2001>.
- Serafini RA, Pryce KD, Zachariou V. The mesolimbic dopamine system in chronic pain and associated affective comorbidities. *Biol Psychiatry* 2020;87:64–73. <https://doi.org/10.1016/j.biopsych.2019.10.018>.
- Hayes DJ, Chen DQ, Zhong J, et al. Affective circuitry alterations in patients with trigeminal neuralgia. *Front Neuroanat* 2017;11:73. <http://journal.frontiersin.org/article/10.3389/fnana.2017.00073/full>.
- Mallory GW, Abulseoud O, Hwang SC, et al. The nucleus accumbens as a potential target for central poststroke pain. *Mayo Clin Proc* 2012;87:1025–1031. <https://doi.org/10.1016/j.mayocp.2012.02.029>.
- Seixas D, Palace J, Tracey I. Chronic pain disrupts the reward circuitry in multiple sclerosis. *Eur J Neurosci* 2016;44:1928–1934. <https://onlinelibrary.wiley.com/doi/10.1111/ejn.13272>.
- Makary MM, Polosecki P, Cecchi GA, et al. Loss of nucleus accumbens low-frequency fluctuations is a signature of chronic pain. *Proc Natl Acad Sci U S A* 2020;117:10015–10023. <https://doi.org/10.1073/pnas.1918682117>.
- Vergara F, Sardi NF, Pescador AC, et al. Contribution of mesolimbic dopamine and kappa opioid systems to the transition from acute to chronic pain. *Neuropharmacology* 2020;178:108226. <https://linkinghub.elsevier.com/retrieve/pii/S002839082030294X>.
- Tracey I, Ploghaus A, Gati JS, et al. Imaging attentional modulation of pain in the periaqueductal gray in humans. *J Neurosci* 2002;22:2748–2752. <https://www.jneurosci.org/lookup/doi/10.1523/JNEUROSCI.22-07-02748.2002>.
- Eippert F, Bingel U, Schoell ED, et al. Activation of the opioidergic descending pain control system underlies placebo analgesia. *Neuron* 2009;63:533–543. <https://doi.org/10.1016/j.neuron.2009.07.014>.
- Hemington KS, Coulombe MA. The periaqueductal gray and descending pain modulation: Why should we study them and what role

- do they play in chronic pain? *J Neurophysiol* 2015;114:2080–2083. <https://doi.org/10.1152/jn.00998.2014>.
23. Denk F, McMahon SB, Tracey I. Pain vulnerability: a neurobiological perspective. *Nat Neurosci* 2014;17:192–200. <https://doi.org/10.1038/nn.3628>.
 24. Arendt-Nielsen L, Morlion B, Perrot S, et al. Assessment and manifestation of central sensitisation across different chronic pain conditions. *Eur J Pain (United Kingdom)* 2018;22:216–241. <https://doi.org/10.1002/ejp.1140>.
 25. Georgopoulos V, Akin-Akinyosoye K, Zhang W, et al. Quantitative sensory testing and predicting outcomes for musculoskeletal pain, disability, and negative affect: a systematic review and meta-analysis. *Pain* 2019;160:1920–1932. <https://journals.lww.com/10.1097/j.pain.0000000000001590>.
 26. Yarnitsky D, Crispel Y, Eisenberg E, et al. Prediction of chronic post-operative pain: pre-operative DNIC testing identifies patients at risk. *Pain* 2008;138:22–28. <https://doi.org/10.1016/j.pain.2007.10.033>.
 27. Millan MJ. The induction of pain: an integrative review. *Prog Neurobiol* 1999;57:1–164. <https://www.sciencedirect.com/science/article/pii/S03041008298000483>.
 28. Millan MJ. Descending control of pain. *Prog Neurobiol* 2002;66:355–474. [https://doi.org/10.1016/S0304-0082\(02\)00009-6](https://doi.org/10.1016/S0304-0082(02)00009-6).
 29. Linnman C, Moulton EA, Barmettler G, et al. Neuroimaging of the periaqueductal gray: State of the field. *Neuroimage* 2012;60:505–522. <https://doi.org/10.1016/j.neuroimage.2011.11.095>.
 30. Yu R, Gollub RL, Spaeth R, et al. Disrupted functional connectivity of the periaqueductal gray in chronic low back pain. *NeuroImage Clin* 2014;6:100–108. <https://doi.org/10.1016/j.nicl.2014.08.019>.
 31. Harper DE, Ichesco E, Schrepf A, et al. Resting functional connectivity of the periaqueductal gray is associated with normal inhibition and pathological facilitation in conditioned pain modulation. *J Pain* 2018;19:635.e1–635.e15. <https://doi.org/10.1016/j.neuroimage.2011.11.095>.
 32. Packard RC. The relationship of neck injury and post-traumatic headache. *Curr Pain Headache Rep* 2002;6:301–307. <http://link.springer.com/10.1007/s11916-002-0051-4>.
 33. Gil C, Decq P. How similar are whiplash and mild traumatic brain injury? A systematic review. *Neurochirurgie* 2021;67:238–243. <https://doi.org/10.1016/j.neuchi.2021.01.016>.
 34. King JA, McCrema MA, Nelson LD. Frequency of primary neck pain in mild traumatic brain injury/concussion patients. *Arch Phys Med Rehabil* 2020;101:89–94. <https://doi.org/10.1016/j.apmr.2019.08.471>.
 35. Lucas S, Hoffman JM, Bell KR, Dikmen S. A prospective study of prevalence and characterization of headache following mild traumatic brain injury. *Cephalalgia* 2013;34:93–102. <https://doi.org/10.1177/0333102413499645>.
 36. van der Naalt J, Timmerman ME, de Koning ME, et al. Early predictors of outcome after mild traumatic brain injury (UPFRONT): an observational cohort study. *Lancet Neurol* 2017;16:532–540. [https://doi.org/10.1016/S1474-4422\(17\)30117-5](https://doi.org/10.1016/S1474-4422(17)30117-5).
 37. Cassidy JD, Boyle E, Carroll LJ. Population-based, inception cohort study of the incidence, course, and prognosis of mild traumatic brain injury after motor vehicle collisions. *Arch Phys Med Rehabil* 2014;95:S278–S285. <https://doi.org/10.1016/j.apmr.2013.08.295>.
 38. Hartvigsen J, Boyle E, Cassidy JD, Carroll LJ. Mild traumatic brain injury after motor vehicle collisions: what are the symptoms and who treats them? A population-based 1-year inception cohort study. *Arch Phys Med Rehabil* 2014;95:S286–S294. <https://doi.org/10.1016/j.apmr.2013.08.295>.
 39. Hoffman JM, Lucas S, Dikmen S, Temkin N. Clinical perspectives on headache after traumatic brain injury. *PM&R* 2020;12:967–974. <https://onlinelibrary.wiley.com/doi/10.1002/pmrj.12338>.
 40. Ashina H, Porreca F, Anderson T, et al. Post-traumatic headache: epidemiology and pathophysiological insights. *Nat Rev Neurol* 2019;15:607–617. <http://www.nature.com/articles/s41582-019-0243-8>.
 41. Cancelliere C, Boyle E, Côté P, et al. Development and validation of a model predicting post-traumatic headache six months after a motor vehicle collision in adults. *Accid Anal Prev* 2020;142:105580. <https://doi.org/10.1016/j.aap.2020.105580>.
 42. Ritchie C, Sterling M. Recovery pathways and prognosis after whiplash injury. *J Orthop Sports Phys Ther* 2016;46:851–861. <http://www.jospt.org/doi/10.2519/jospt.2016.6918>.
 43. Newbold DJ, Laumann TO, Hoyt CR, et al. Plasticity and spontaneous activity pulses in disused human brain circuits. *Neuron* 2020;107:580–589.e6. <https://doi.org/10.1016/j.neuron.2020.05.007>.
 44. Gratton C, Laumann TO, Nielsen AN, et al. Functional brain networks are dominated by stable group and individual factors, not cognitive or daily variation. *Neuron* 2018;98:439–452.e5. <https://doi.org/10.1016/j.neuron.2018.03.035>.
 45. Kuperman P, Granovsky Y, Granot M, et al. Psychophysical dichotomy in very early acute mTBI pain. *Neurology* 2018;91:e931–e938. <https://doi.org/10.1212/WNL.0000000000006120>.
 46. Al-Khazali HM, Ashina H, Iljazi A, et al. Neck pain and headache after whiplash injury: a systematic review and meta-analysis. *Pain* 2020;161:880–888. https://journals.lww.com/pain/Fulltext/2020/05000/Neck_pain_and_headache_after_whiplash_injury__a.2.aspx.
 47. Beeckmans K, Crunelle C, Van Ingelgom S, et al. Persistent cognitive deficits after whiplash injury: a comparative study with mild traumatic brain injury patients and healthy volunteers. *Acta Neurol Belg* 2017;117:493–500. <https://doi.org/10.1007/s13760-017-0745-3>.
 48. Spitzer WO, Skovron ML, Salmi LR, et al. Scientific monograph of the Quebec Task Force on Whiplash-Associated Disorders: redefining “whiplash” and its management. *Spine* 1995;20:1S–73S. <http://europepmc.org/abstract/MED/7604354>.
 49. Moore RA, Straube S, Aldington D. Pain measures and cut-offs – ‘no worse than mild pain’ as a simple, universal outcome. *Anaesthesia* 2013;68:400–412. <https://doi.org/10.1111/anae.12148>.
 50. Power JD, Mitra A, Laumann TO, et al. Methods to detect, characterize, and remove motion artifact in resting state fMRI. *Neuroimage* 2014;84:320–341. <https://doi.org/10.1016/j.neuroimage.2013.08.048>.
 51. Kahn I, Andrews-Hanna JR, Vincent JL, et al. Distinct cortical anatomy linked to subregions of the medial temporal lobe revealed by intrinsic functional connectivity. *J Neurophysiol* 2008;100:129–139. <http://www.pubmedcentral.nih.gov/articlerender.fcgi?artid=2493488&tool=pmcentrez&rendertype=abstract>.
 52. Rieckmann A, Johnson KA, Sperling RA, et al. Dedifferentiation of caudate functional connectivity and striatal dopamine transporter density predict memory change in normal aging. *Proc Natl Acad Sci* 2018;115:10160–10165. <https://pnas.org/doi/full/10.1073/pnas.1804641115>.
 53. Siman-Tov T, Bosak N, Sprecher E, et al. Early age-related functional connectivity decline in high-order cognitive networks. *Front Aging Neurosci* 2017;8:330. <https://doi.org/10.3389/fnagi.2016.00330>.
 54. Li J, Kong R, Liégeois R, et al. Global signal regression strengthens association between resting-state functional connectivity and behavior. *Neuroimage* 2019;196:126–141. <https://doi.org/10.1016/j.neuroimage.2019.04.016>.
 55. Coulombe MA, Erpelding N, Kucyi A, Davis KD. Intrinsic functional connectivity of periaqueductal gray subregions in humans. *Hum Brain Mapp* 2016;37:1514–1530. <http://dx.doi.org/10.1002/hbm.23117>.
 56. Saadon-Grosman N, Loewenstein Y, Arzy S. The ‘creatures’ of the human cortical somatosensory system. *Brain Commun* 2020;2:fcaa003. <http://dx.doi.org/10.1093/braincomms/fcaa003>.

57. Pedregosa F, Varoquaux G, Gramfort A, et al. Scikit-learn: machine learning in Python. *J Mach Learn Res* 2011;12:2825–2830. <https://doi.org/10.48550/arXiv.1201.0490>.
58. Xia X, Fan L, Cheng C, et al. Multimodal connectivity-based parcellation reveals a shell-core dichotomy of the human nucleus accumbens. *Hum Brain Mapp* 2017;38:3878–3898. <http://dx.doi.org/10.1002/hbm.23636>.
59. Penfield W, Boldrey E. Somatic motor and sensory representation in the cerebral cortex of man as studied by electrical stimulation. *Brain A J Neurol* 1937;60:389–443. <https://doi.org/10.1093/brain/60.4.389>.
60. Rolls ET, Huang CC, Lin CP, et al. Automated anatomical labelling atlas 3. *Neuroimage* 2020;206:116189. <https://doi.org/10.1016/j.neuroimage.2019.116189>.
61. Mogenson GJ, Jones DL, Yim CY. From motivation to action: functional interface between the limbic system and the motor system. *Prog Neurobiol* 1980;14:69–97. <https://www.sciencedirect.com/science/article/pii/030100828090018062>.
62. Li H, Li X, Feng Y, et al. Deficits in ascending and descending pain modulation pathways in patients with postherpetic neuralgia. *Neuroimage* 2020;221:117186. <https://doi.org/10.1016/j.neuroimage.2020.117186>.
63. Tu Y, Fu Z, Mao C, et al. Distinct thalamocortical network dynamics are associated with the pathophysiology of chronic low back pain. *Nat Commun* 2020;11:1–12. <https://doi.org/10.1038/s41467-020-17788-z>.
64. Cummiford CM, Nascimento TD, Foerster BR, et al. Changes in resting state functional connectivity after repetitive transcranial direct current stimulation applied to motor cortex in fibromyalgia patients. *Arthritis Res Ther* 2016;18:1–12. <https://doi.org/10.1186/s13075-016-0934-0>.
65. Ma QP, Shi YS, Han JS. Further studies on interactions between periaqueductal gray, nucleus accumbens and habenula in antinociception. *Brain Res* 1992;583:292–295. [https://doi.org/10.1016/s0006-8993\(10\)80036-8](https://doi.org/10.1016/s0006-8993(10)80036-8).
66. Stevens FL, Hurley RA, Taber KH. Anterior cingulate cortex: unique role in cognition and emotion. *J Neuropsychiatry Clin Neurosci* 2011;23:121–125. <https://doi.org/10.1176/jnp.23.2.jnp121>.
67. Ayoub LJ, McAndrews MP, Barnett AJ, et al. Baseline resting-state functional connectivity determines subsequent pain ratings to a tonic ecologically valid experimental model of orofacial pain. *Pain* 2021; 162:2397–2404. <https://doi.org/10.1097/j.pain.0000000000002225>.
68. Li Z, Liu M, Lan L, et al. Altered periaqueductal gray resting state functional connectivity in migraine and the modulation effect of treatment. *Sci Rep* 2016;6:20298. <https://doi.org/10.1038/srep20298>.
69. Tovar DT, Chavez RS. Large-scale functional coactivation patterns reflect the structural connectivity of the medial prefrontal cortex. *Soc Cogn Affect Neurosci* 2021;16:875–882. <https://academic.oup.com/scan/article/16/8/875/5912489>.